INVITED PAPER

Bianisotropic Effective Parameters of Optical Metamagnetics and Negative-Index Materials

An overview of some principles in development of bianisotropic homogenization techniques for metamaterials is given in this paper with examples in passive and active optical metamaterials.

By Alexander V. Kildishev, *Senior Member IEEE*, Joshua D. Borneman, Xingjie Ni, Vladimir M. Shalaev, *Fellow IEEE*, and Vladimir P. Drachev

ABSTRACT | Approaches to the adequate homogenization of optical metamaterials are becoming more and more complex, primarily due to an increased understanding of the role of asymmetric electrical and magnetic responses, in addition to the nonlocal effects of the surrounding medium, even in the simplest case of plane-wave illumination. The current trend in developing such advanced homogenization descriptions often relies on utilizing bianisotropic models as a base on top of which novel optical characterization techniques can be built. In this paper, we first briefly review general principles for developing a bianisotropic homogenization approach. Second, we present several examples validating and illustrating our approach using single-period passive and active optical metamaterials. We also show that the substrate may have a significant effect on the bianisotropic characteristics of otherwise symmetric passive and active metamaterials.

KEYWORDS | Bianisotropic media; homogenization; metamagnetics; metamaterials

Manuscript received June 20, 2010; revised May 29, 2011; accepted June 19, 2011. Date of publication August 12, 2011; date of current version September 21, 2011. This work was supported in part by the U.S. Army Research Office Multidiciplinary University Research Initiative (ARO-MURI) under Grants 50342-PH-MUR and W911NF-09-1-0539 and by the U.S. Office of Naval Research (ONR) under Grant N000014-10-1-0942.

A. V. Kildishev, **X. Ni**, **V. M. Shalaev**, and **V. P. Drachev** are with the Birck Nanotechnology Center, School of Electrical and Computer Engineering, Purdue University, West Lafayette, IN 47907 USA (e-mail: a.v.kildishev@ieee.org).

J. D. Borneman was with the Birck Nanotechnology Center, School of Electrical and Computer Engineering, Purdue University, West Lafayette, IN 47907 USA. He is now with NSWC Crane Division, Crane, IN 47522 USA.

Digital Object Identifier: 10.1109/JPROC.2011.2160991

I. INTRODUCTION

A new class of nanostructured materials (often called optical metamaterials) makes it possible to achieve optical properties that do not exist in nature [1]. Predicting and describing the effective behavior of optical metamaterials in general requires knowledge of their wavevector- and wavelength-dependent dispersion [2]. Upon plane wave excitation though, the effective properties of a thin metamaterial layer can be evaluated using a standard homogenization approach [3]–[5], which approximates a nanostructure with a homogeneous layer equivalently producing the same complex transmission and reflection coefficients at normal incidence. However, in actual nanostructured optical metamaterials, due to realistic fabrication tolerances and the necessity for mechanical support with a single- or multilayer substrate, the geometry will inevitably become asymmetric, causing different reflections and even transmissions upon front-side and back-side illumination.

This paper deals with the theoretical fundamentals of bianisotropic homogenization, as it applies to passive and active optical metamaterials (MMs). It reviews the basic structure of 2-D optical metamagnetic and negative-index materials (Section II) and presents the details of the mathematical apparatus behind a particular case of bianisotropic homogenization upon normal incidence of light (Section III) for a general nonreciprocal material. The paper then examines the spectral dependencies of their retrieved effective parameters (Section V). A special effort

is made to analyze the influence of the substrate on otherwise symmetric structures. Numerical and analytical techniques for validating the proposed approach are additionally discussed in Section IV, where a special case of reciprocal media is considered.

Since the structural asymmetries are not incorporated into a standard homogenization scheme, their effects on the electromagnetic properties cannot be directly employed in a wave dynamics model even at the simplest case of plane wave excitation. Challenges in retrieving the effective properties also arise with when embedding gain materials, as the magnitude of the gain grows and the influence of the asymmetries on active modes becomes increasingly important, just because the standard homogenization only accounts for symmetric intrinsic impedances, and the parameters it predicts at elevated gain levels could be overestimated.

II. METAMAGNETICS AND NEGATIVE-INDEX MATERIALS

This section deals with single-period optical MMs, including optical metamagnetics and negative-index materials. For the time being it suffices to state that the wave equation of such structures allows for 2-D scalar implementation, where the TM case (the single component of the magnetic field is perpendicular to the propagation direction of the incident light and to the periodicity direction) is of prime interest here.

Optical metamagnetics (OMs) are a class of artificially fabricated optical materials (MM) that are designed to produce a strong magnetic response at optical frequencies. OMs can be obtained, for example, using 1-D subwavelength-periodic arrays of nanofabricated silver strip pairs separated by a dielectric spacer as shown in Fig. 1(a). These structures exhibit unusual (artificial) magnetism, not available in nature at the optical range. Studies of OMs have been an important part of MM research [1], [6]–[17] in the area of optical MMs because no negative-index material is achievable without an artificial magnetic response (due to the necessary condition for obtaining a negative index) [18], [19].

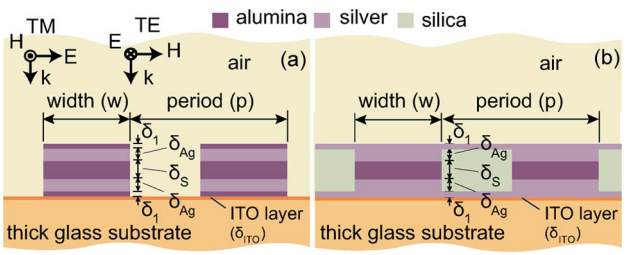

Fig. 1. ***The cross sections (a) of a typical metamagnetic and (b) of an example 2-D negative-index material.***

Negative-index metamaterials (NIMs) are yet another class of optical MMs that are designed to produce negative refraction, axis-free imaging, super resolution, and other effects [20]. In the simplest case of an effectively uniform medium, control of the electromagnetic waves is thought to be accomplished through the effective permittivity μ and permeability ε [21], [22]. The effective μ and ε is a result of some averaging of the intrinsic parameters, permittivity, and permeability, in electromagnetic MMs. Related to this is the mechanics of wave propagation in hyperbolic MMs or indefinite index media [23]–[27] and more general MMs based on the transformation optics (TO) concept [17], [28], [29]. So called double-negative NIMs are passive MMs with simultaneously negative real parts of μ and ε, in contrast with single-negative NIMs where only the real part of ε is negative.

Along with a popular fishnet design [1], [30], [31], an alternative structure, shown in Fig. 1(b), could serve the same purpose. Thus, this paper deals with a double-negative NIM arranged as a combination of a 2-D metamagnetic with two continuous metal films [Fig. 1(b)] [7]. Although an optimal design proposed in [28] required previously challenging fabrication of ultrathin films, this drawback now can be readily alleviated by using a Ge wetting technique resulting in low-loss ultrathin Ag films [32], [33].

III. BIANISOTROPIC HOMOGENIZATION

A very first method for improving the homogenized MM description is to use bianisotropy (BA) for the material description of the effective slab [34]–[38]. This approach takes into account the nonreciprocal reflection of asymmetric MMs and simultaneously accounts for combined symmetric and asymmetric electric responses, so that some difficulties in the effective characterization of OMs are alleviated.

This section presents the fundamentals of the BA homogenization, provided that only normally incident light is used. The homogenization for a realistic case of MMs deposited on a covered substrate are discussed here.

The study done by Chen *et al.* [36] deals with the intrinsically asymmetric unit cell structure placed in free space without any super- or substrate. Another asymmetric unit cell structure (in the presence of a uniform substrate and associated nonlocal effects) is rigorously analyzed in related works [35], [39], and [40]. In contrast to those studies: 1) we show that the nonlocal effects of the substrate are quite important even for ideally symmetric unit cell, and cannot be ignored especially in thin samples; 2) we introduce an additional thin adhesion layer into the retrieval of BA parameters; and finally and most important, 3) we show that the resulting effective BA slab on a substrate can be alternatively described by unidirectional gradients of the complex permittivity $\tilde{\varepsilon}(x)$ and permeability $\tilde{\mu}(x)$, which are different for the front-side or back-side

illumination. A less general version of our retrieval technique has been used for the numerical analysis and experimental demonstration of active optical MM with negative index of refraction [41].

A. Effective Parameters of a Bianisotropic Slab

Throughout the paper the monochromatic time-dependent terms $e^{-\iota\omega t}$ are omitted and the free-space parameters λ_0, $k_0 = 2\pi/\lambda_0$, $c_0 = 1/\sqrt{\varepsilon_0\mu_0}$, $z_0 = \sqrt{\mu_0}/\sqrt{\varepsilon_0}$, ε_0, and μ_0, respectively, denote the wavelength, the wavenumber, the velocity of light, the intrinsic impedance, the permittivity, and the permeability.

For the TM case, we define the fields $\mathbf{E} = \hat{\mathbf{y}}e_y$, $\mathbf{H} = \hat{\mathbf{z}}h_z$, $\mathbf{D} = \hat{\mathbf{y}}d_y$, $\mathbf{B} = \hat{\mathbf{z}}b_z$; then, using a matrix notation as

$$\mathbf{f} = \begin{pmatrix} e_y \\ h_z \end{pmatrix} \quad \mathbf{d} = \begin{pmatrix} d_y \\ b_z \end{pmatrix} \tag{1}$$

and introducing the curl operator $\mathbf{c} = \mathbf{i}_r\partial_x$, and the BA material matrix $\mathbf{m}$, we combine the Maxwell curl equations into a matrix form

$$\partial\mathbf{d}/\partial t = \iota k_0 \mathbf{m}\cdot\mathbf{f} = \mathbf{c}\cdot\mathbf{f} \tag{2}$$

with $\mathbf{i}_r = \begin{pmatrix} 0 & 1 \\ 1 & 0 \end{pmatrix}$, and $\mathbf{m} = \begin{pmatrix} z_0^{-1}\varepsilon & u \\ v & z_0\mu \end{pmatrix}$, where the material matrix $\mathbf{m}$, along with relative permittivity ε and relative permeability μ, includes bianosotropic parameters u, v.

The electric field inside the BA slab (see Fig. 2) can be written as the forward wave $(e_{13} = a_{13}e^{\iota k_0 n_{13}x})$, and the backward wave $(e_{31} = a_{31}e^{-\iota k_0 n_{31}x})$, and following the formalism of (1), we may now define the field in the slab as

$$\mathbf{f}_{13} = \begin{pmatrix} 1 \\ z_0^{-1}z_{13}^{-1} \end{pmatrix} a_{13}e^{\iota k_0 n_{13}x} \quad \mathbf{f}_{31} = \begin{pmatrix} 1 \\ -z_0^{-1}z_{31}^{-1} \end{pmatrix} a_{31}e^{-\iota k_0 n_{31}x} \tag{3}$$

where z_{13}, n_{13} and z_{31}, n_{31} are the impedance and the refractive index for the forward and backward waves, respectively—another set of BA parameters that should be linked to the terms of matrix $\mathbf{m}$.

First, using (2), we arrive at the dispersion identities

$$(\mathbf{m} - n_{13}\mathbf{i}_r)\cdot\mathbf{f}_{13} = 0 \quad (\mathbf{m} + n_{31}\mathbf{i}_r)\cdot\mathbf{f}_{31} = 0 \tag{4}$$

where in order to satisfy the Maxwell equations the following identities should initially hold:

$$z_{13} = \varepsilon^{-1}(n_{13} - u) \quad z_{31} = \varepsilon^{-1}(n_{31} + u). \tag{5}$$

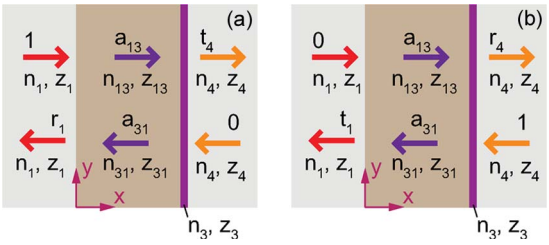

Fig. 2. ***Propagation through a bianisotropic slab*** $(0 \le x \le x_0)$***, characterized by*** n_{13}, z_{13} ***and*** n_{31}, z_{31}***, the impedance and the refractive index of the forward and backward waves, respectively. The slab is covered by a semi-infinite superstrate layer*** $(x \le 0, n_1, z_1)$ ***and is deposited on a cover layer*** $(x_o < x < x_b, n_3, z_3)$ ***placed on top of semi-infinite superstrate layer*** $(x_b < x, n_4, z_4)$***. (a) Illumination from the superstrate side. (b) Illumination from the substrate side.***

Then, from (4), we arrive at

$$|\mathbf{m} - n_{13}\mathbf{i}_r| = 0 \quad |\mathbf{m} + n_{31}\mathbf{i}_r| = 0. \tag{6}$$

Thus, solving (6), we have

$$\varepsilon\mu = (n_{13} - v)(n_{13} - u) = (n_{31} + v)(n_{31} + u) \tag{7}$$

and we may write

$$n_{13} = \frac{1}{2}\left(\pm\sqrt{4\varepsilon\mu + (u - v)^2} + u + v\right)$$
$$n_{31} = \frac{1}{2}\left(\pm\sqrt{4\varepsilon\mu + (u - v)^2} - u - v\right). \tag{8}$$

We will note an important reduction obtained directly from (8), first by multiplying the solutions, and then by subtracting them

$$n_{13}n_{31} = \varepsilon\mu - uv \quad n_{13} - n_{31} = u + v. \tag{9}$$

Finally, provided that $n_{13} \neq n_{31}$ and $z_{13} \neq z_{31}$ are given, the effective parameters ε, μ, u, and v are obtained first from (7), and (9)

$$\varepsilon = (n_{13} + n_{31})/(z_{13} + z_{31})$$
$$u = \varepsilon(n_{13}z_{31} - n_{31}z_{13})/(n_{13} + n_{31})$$
$$v = n_{13} - n_{31} - u$$
$$\mu = (n_{13}n_{31} + uv)/\varepsilon. \tag{10}$$

The above defines the sequence of conversion from parameters z_{13}, n_{13} and z_{31}, n_{31}—which are available from experiment—to unknown parameters u, v, μ, and ε. The particular case of $u = -v$ matches [35], [39].

Using the notation of (3), the fields can be defined in the following regions: fields in the *superstrate layer* (region $x < 0$) can be expressed as $\mathbf{f}_1(x) = \mathbf{z}_0^{-1}\mathbf{z}_1^{-1}\mathbf{u}\mathbf{s}_1\mathbf{a}_1$, fields in the *BA layer* (region $0 \le x \le x_0$) can be expressed as $\mathbf{f}_2(x) = \mathbf{z}_0^{-1}\mathbf{v}_2\mathrm{diag}(z_{13}, z_{31})^{-1}\mathbf{s}_2\mathbf{a}_2$, fields in the *cover layer* (region $x_0 < x \le x_c$) can be expressed as $\mathbf{f}_3(x) = \mathbf{z}_0^{-1}\mathbf{z}_3^{-1}\mathbf{u}\mathbf{s}_3\mathbf{a}_3$, and fields in the *substrate layer* (region $x_c < x$) can be expressed as $\mathbf{f}_4(x) = \mathbf{z}_0^{-1}\mathbf{z}_4^{-1}\mathbf{u}\mathbf{s}_4\mathbf{a}_4$, where

$$\begin{aligned}
&\mathbf{s}_1 = \mathrm{diag}\left(s_1, s_1^{-1}\right) \quad s_1 = e^{\iota k_0 n_1 x} \quad \mathbf{s}_2 = \mathrm{diag}(s_{13}, s_{31})\\
&s_{13} = e^{\iota k_0 n_{13} x} \qquad s_{31} = e^{\iota k_0 n_{31} x}\\
&\mathbf{s}_3 = \mathrm{diag}(s_3, s_3^{-1}) \quad s_3 = e^{\iota k_0 n_3 x}\\
&\mathbf{s}_4 = \mathrm{diag}\left(s_4, s_4^{-1}\right) \quad s_4 = e^{\iota k_0 n_4 x}\\
&\mathbf{z}_i = \mathrm{diag}(1, z_i), \qquad i = 0, 1, 3, 4
\end{aligned}$$

and

$$\mathbf{u} = \begin{pmatrix} 1 & 1 \\ 1 & -1 \end{pmatrix} \quad \mathbf{v}_2 = \begin{pmatrix} z_{13} & z_{31} \\ 1 & -1 \end{pmatrix} \quad \mathbf{a}_1 = \begin{pmatrix} a_{12} \\ a_{21} \end{pmatrix}$$
$$\mathbf{a}_2 = \begin{pmatrix} a_{13} \\ a_{31} \end{pmatrix} \qquad \mathbf{a}_3 = \begin{pmatrix} a_{23} \\ a_{32} \end{pmatrix} \qquad \mathbf{a}_4 = \begin{pmatrix} a_{34} \\ a_{43} \end{pmatrix}.$$

Using the standard boundary conditions

$$\mathbf{z}_1^{-1}\mathbf{u}\mathbf{a}_1 = \mathbf{v}_2\mathrm{diag}(z_{13}, z_{31})^{-1}\mathbf{s}_2\mathbf{a}_2$$
$$\mathbf{a}_2 = \left[\mathbf{v}_2\mathrm{diag}(z_{13}, z_{31})^{-1}\mathbf{s}_2(x_0)\right]^{-1}\mathbf{z}_3^{-1}\mathbf{u}\mathbf{s}_3(x_0)\mathbf{a}_3 \quad (11)$$
$$\mathbf{a}_3 = \left[\mathbf{z}_3^{-1}\mathbf{u}\mathbf{s}_3(x_c)\right]^{-1}\mathbf{z}_4^{-1}\mathbf{u}\mathbf{s}_4(x_c)\mathbf{a}_4 \quad (12)$$

we obtain

$$\mathbf{t}\mathbf{z}_1^{-1}\mathbf{u}\mathbf{a}_1 = \mathbf{t}_3^{-1}\mathbf{z}_4^{-1}\mathbf{u}\tilde{\mathbf{a}}_4 \quad (13)$$

where $\mathbf{t}_3 = \mathbf{z}_3^{-1}\mathbf{u}\mathbf{s}_3(x_c - x_0)\mathbf{u}^{-1}\mathbf{z}_3$, $\tilde{\mathbf{a}}_4 = \mathbf{s}_4(x_c)\mathbf{a}_4$, then

$$\mathbf{z}_4\mathbf{t}_3\mathbf{t}\mathbf{z}_1^{-1}\begin{pmatrix} a_{12} + a_{21} \\ a_{12} - a_{21} \end{pmatrix} = \begin{pmatrix} \tilde{a}_{34} + \tilde{a}_{43} \\ \tilde{a}_{34} - \tilde{a}_{43} \end{pmatrix} \quad (14)$$

and hence, the transfer matrix is

$$\mathbf{t} = \mathbf{v}_2\mathbf{s}_2(x_0)\mathbf{v}_2^{-1}. \quad (15)$$

Dividing the field magnitudes in (14) either by the superstrate side incident magnitude a_{12}, or by the substrate side incident magnitude $\tilde{a}_{43}$, we arrive at

$$\mathbf{t}\mathbf{z}_1^{-1}\begin{pmatrix} 1 + r_1 \\ 1 - r_1 \end{pmatrix} = \mathbf{t}_3^{-1}\mathbf{z}_4^{-1}\begin{pmatrix} t_4 \\ t_4 \end{pmatrix}$$
$$\mathbf{t}\mathbf{z}_1^{-1}\begin{pmatrix} t_1 \\ -t_1 \end{pmatrix} = \mathbf{t}_3^{-1}\mathbf{z}_4^{-1}\begin{pmatrix} r_4 + 1 \\ r_4 - 1 \end{pmatrix} \quad (16)$$

to finally get the transfer matrix connection

$$\mathbf{t} = \mathbf{t}_3^{-1}\mathbf{z}_4^{-1}\mathbf{w}\mathbf{z}_1$$
$$\mathbf{w} = \begin{pmatrix} t_4 & r_4 + 1 \\ t_4 & r_4 - 1 \end{pmatrix}\begin{pmatrix} 1 + r_1 & t_1 \\ 1 - r_1 & -t_1 \end{pmatrix}^{-1}. \quad (17)$$

Now, we need to convert (17) into (15) using factorization, thus obtaining z_{13}, z_{31}, s_{13}, and s_{31} through one to one comparison. To perform such eigendecomposition, we write the transfer matrix as

$$\mathbf{t} = \begin{pmatrix} \mathbf{t}_{11} & \mathbf{t}_{12} \\ \mathbf{t}_{21} & \mathbf{t}_{22} \end{pmatrix} \quad (18)$$

and after bringing in auxiliary parameters σ, δ, τ^2, and Δ

$$\delta = \mathbf{t}_{11} - \mathbf{t}_{22} \quad \tau^2 = 4\mathbf{t}_{12}\mathbf{t}_{21}$$
$$\sigma = \mathbf{t}_{11} + \mathbf{t}_{22} \quad \Delta = \pm\sqrt{\sigma^2 + \tau^2} \quad (19)$$

the factorization of (17) gives the analog of (15), with

$$\mathbf{v}_2 = \begin{pmatrix} (\delta - \Delta)/(2\mathbf{t}_{21}) & (-\delta - \Delta)/(2\mathbf{t}_{21}) \\ 1 & -1 \end{pmatrix}. \quad (20)$$

Then, the diagonal terms of $\mathbf{s}_2$ can be obtained from

$$s_{13} = \frac{1}{2}(\sigma - \Delta) \quad s_{31} = \frac{1}{2}(\sigma + \Delta). \quad (21)$$

Finally, the effective parameters of the BA slab are

$$n_{13} = (k_0 x_0)^{-1} \cos^{-1}\left(\frac{1}{2}[s_{13} + 1/s_{13}]\right)$$

$$n_{31} = (k_0 x_0)^{-1} \cos^{-1}\left(\frac{1}{2}[s_{31} + 1/s_{31}]\right) \quad (22)$$

$$z_{13} = (\delta - \Delta)/(2\mathbf{t}_{21}),\ z_{31} = (-\delta - \Delta)/(2\mathbf{t}_{21}). \quad (23)$$

Once the values of n_{13}, n_{31}, z_{13}, and z_{31} are obtained from the measured complex transmission and reflection coefficients, the effective parameters ε, μ, u, and v are retrieved using (10). An appropriate branch in (22) and (23) should be selected using the conventional restriction [2], [34]–[36] for passive MMs. For the active MMs examined in this paper, maintaining the continuity of $\mathrm{Re}(n)$ and $\mathrm{Im}(n)$ produced straightforward retrievals.

B. Numerical Modeling of a Bianisotropic Slab

It is also desirable to model BA samples using, for example, 2-D (scalar) finite element TM solvers. We consider a propagating H-field inside a BA slab as $h_j = h_{13,j} = h_{31,j}$; E-field is then $e_j = z_0(z_{13}h_{13,j} - z_{31}h_{31,j})$, where index j denotes either superstrate-side (i.e., front-side f) or substrate-side (i.e., back-side b) illumination, as shown in Fig. 1. To separate the waves within the slab we have to write the identities for the forward (24) and backward (25) waves $(j = f, b)$

$$h_{13,j} = (k_0 n_{31} h_j - \iota \partial h_j/\partial x)/[k_0(n_{13} + n_{31})] \quad (24)$$

$$h_{31,j} = (k_0 n_{13} h_j + \iota \partial h_j/\partial x)/[k_0(n_{13} + n_{31})]. \quad (25)$$

Then, the magnetic flux density $b_j = b_{13,j} + b_{31,j}$ and the displacement vector $d_j = d_{13,j} + d_{31,j}$ can be obtained from (2) using $\mathbf{m}$ as

$$d_j = c_0^{-1}\left[(z_{13}\varepsilon + u)h_{13,j} - (z_{31}\varepsilon - u)h_{31,j}\right]$$

$$b_j = \mu_0\left[(\mu + z_{13}v)h_{13,j} + (\mu - z_{31}v)h_{31,j}\right]. \quad (26)$$

If we consider a general definition of inhomogeneous optical material parameters as the ratio between the magnetic flux and the magnetic field, or between the displacement vector and the electric field, then we may express the inhomogeneous relative permittivity $\tilde{\mu}_j$ and permeability $\tilde{\varepsilon}_j$ for the bianisotropic TM model as

$$\tilde{\mu}_j = b_j/(\mu_0 h_j) \quad \tilde{\varepsilon}_j = d_j/(\varepsilon_0 e_j) \quad (27)$$

and as before j denotes either superstrate-side (f) or subtstrate-side (b) illumination (for the particular cases considered here, due to the periodic symmetry, the effective inhomogeneous parameters $\tilde{\mu}_j$ and $\tilde{\varepsilon}_j$ change only along the propagation direction). Equations (27) together with (24) and (25) are used as auxiliary differential equations that are solved consistently within a shared FE computational domain using a commercial FE software (COMSOL Multiphysics).

This approach is also addressing vital questions on 1) how (and whether it is even possible) to get an effective description of an MM using the unique distributions of only two gradient parameters $\tilde{\mu}_j(x)$ and $\tilde{\varepsilon}_j(x)$, and hence, 2) if those distributions could be physically realized to substitute the entire BA slab. As we show later on, the intuitively negative answer to 2) also comes from the fact that even for reciprocal BA media $\tilde{\mu}_f \neq \tilde{\mu}_b$ and $\tilde{\varepsilon}_f \neq \tilde{\varepsilon}_b$.

Alternatively, the validation can also be performed analytically. The coefficients of the fields inside the BA slab a_{13} and a_{31} may be obtained by using (11) and (12). The coefficients of the fields in the substrate for the front-side and back-side illumination are expressed as $\tilde{a}_4 = (t_4, 0)^T$ and $\tilde{a}_4 = (r_4, 1)^T$, respectively. Therefore, the fields inside the BA slab are known due to (3). Then, the electric displacement and the magnetic flux density inside the BA slab can be obtained using (2). Hence, after getting the total field by superimposing the forward and backward waves, the inhomogeneous relative permittivity $\tilde{\mu}$ and $\tilde{\varepsilon}$ permeability for the BA slab can be obtained from (27).

This section gives a homogenization approach pertinent to the characterization of a general, either reciprocal or nonreciprocal thin MM sample deposited on a coated substrate and illuminated with normally incident light. The sequence of conversion from measured complex parameters t_1, t_4 and r_1, r_4—which are available from experiment—to unknown effective parameters z_{13}, n_{13} and z_{31}, n_{31} is given as follows. First, all the elements of matrix $\mathbf{t}$ are obtained from (17); then, those entries ($\mathbf{t}_{11}$, $\mathbf{t}_{12}$, $\mathbf{t}_{21}$, and $\mathbf{t}_{22}$) are used to get the auxiliary parameters σ, δ, τ^2, and Δ from (19) and retrieve the elements of $\mathbf{s}_2 = \mathrm{diag}(s_{13}, s_{31})$ from (21). Finally, using s_{13}, s_{31}, and $\mathbf{t}_{21}$, the auxiliary parameters δ and Δ, the effective parameters n_{13}, n_{31} and z_{13}, z_{31} can be obtained from (22) and (23). An alternative set of the effective BA parameters ε, μ, u, and v is retrieved using (10).

In contrast with constant and illumination-side independent sets of effective parameters $\{n_{13}, n_{31}, z_{13}, z_{31}\}$ or $\{\varepsilon, \mu, u, v\}$, an important notion of the effective permittivity $\tilde{\varepsilon}_j$ and permeability $\tilde{\mu}_j$ is introduced in this section. Equations (24)–(27), defining $\tilde{\varepsilon}_j$ and $\tilde{\mu}_j$ (with j being either superstrate-side f or subtstrate-side b illumination) are obtained using the Sommerfeld splitting. Due to the normal incidence and the periodic symmetry, the inhomogeneous parameters $\tilde{\mu}_j$ and $\tilde{\varepsilon}_j$ change only along the propagation direction, and as we also show in Section V, are illumination-side dependent.

IV. BIANISOTROPIC RECIPROCAL MEDIA

This section covers an important case of reciprocal media followed by the reciprocity-induced simplifications to the general BA homogenization shown in Section III. Here, all discussions and simulations are dealing with reciprocal media, which are of the most interest for the BA characterization of thin MM samples in optics.

In reciprocal media the power transmission is independent of the illumination side, so that the intensity of light transmitted from to the left $T_1 = t_1^2 z_4 z_1^{-1}$ is equal to the intensity transmitted to the right $T_4 = t_4^2 z_1 z_4^{-1}$ (see Fig. 2); here, the illumination-side impedances are used to normalize the incident power. As $z_4 z_1^{-1} = t_4 t_1^{-1} = |\mathbf{w}|$, $|\mathbf{z}_4| = z_4$, $|\mathbf{z}_1^{-1}| = z_1^{-1}$, $|\mathbf{t}_3| = 1$, and as from (17), we have $|\mathbf{z}_4||\mathbf{t}_3||\mathbf{t}||\mathbf{z}_1^{-1}| = z_4 z_1^{-1}$, we finally arrive at the requirement that the matrix $\mathbf{t}$ is simplectic, i.e., $|\mathbf{t}| = (1/4)(\sigma^2 - \Delta^2) = 1$. As a result, $\mathbf{s}_2$ will be a symplectic matrix as well ($|\mathbf{s}_2| = s_{13}s_{31} \equiv 1$). That means that the propagation constants are identical for both directions ($n_{13} = n_{31}$) and do not depend on the illumination side. Then, the retrieval (22) and (23) for a reciprocal medium will degenerate into ($s_{13} = s_{31} \to s$, $n_{13} = n_{31} \to n$, and $u = -v$)

$$n = (k_0 x_0)^{-1} \cos^{-1}\left[\frac{1}{2}(s + s^{-1})\right] \tag{28}$$

$$z_{13} = (\delta - \Delta)/(2\mathbf{t}_{21}),\ z_{31} = (-\delta - \Delta)/(2\mathbf{t}_{21}) \tag{29}$$

and $z_{13}z_{31} = \mathbf{t}_{12}/\mathbf{t}_{21}$.

In contrast with Section III, dealing with a more general case, the BA parameters for reciprocal media are given by much simpler formulas

$$\varepsilon = n\frac{2}{z_{13}+z_{31}} \quad \mu = n\frac{2}{z_{13}^{-1}+z_{31}^{-1}} \quad u = n\frac{z_{31}-z_{13}}{z_{13}+z_{31}} \tag{30}$$

with a more straightforward analogy to a homogeneous slab.

Thus, effective permittivity ε is defined as a ratio of effective index n to averaged effective impedances, effective permittivity μ is given by the ratio of n to the averaged admittances, while BA parameter u is given as a product of n with a relative difference in effective z_{31} and z_{13}.

V. EXAMPLE RETRIEVAL FOR RECIPROCAL MEDIA

Here we examine the results of the BA homogenization method on several example geometries. Electromagnetic simulations of these geometries were done using a 2-D spatial harmonic analysis (SHA) method [42], [43] for both front-side and back-side illumination, resulting in complex transmission (t_1, t_4) and reflection (r_1, r_4) coefficients. Equations (28), (29), and (30) are then used to determine the effective BA parameters of the MM. In order to validate these results, we then obtain the complex transmission and reflection coefficients of a homogeneous bianisotropic slab with a permittivity and permeability as defined in (27), using FE model described above. As we will show, the coefficients t_1, t_4 and r_1, r_4 obtained from the homogenized BA slab match those of structured MM, successfully validating the retrieved effective parameters.

First, we examine a simple metamagnetic grating, as shown in Fig. 1(a). The upper and lower dielectric layers and the indium tin oxide (ITO) layer are usually present due to fabrication requirements, and are not necessary to the fundamental performance of the metamagnetic, therefore we have removed these layers $\delta_1 = \delta_{\mathrm{ITO}} = 0$ in order to examine the core three-layer metamagnetic. The remaining geometric dimensions are $\{p, w, \delta_{\mathrm{Ag}}, \delta_{\mathrm{s}}\} = \{250, 120, 30, 40\}$ [nm]. The SHA simulation results are given as the wavelength-dependent phasor diagrams of complex r, t coefficients in Fig. 3(a) and (b), for front-side and back-side illumination, respectively. As expected for a reciprocal medium, the substrate-normalized values of t coefficients shown as black solid lines in Fig. 3(a) and (b) are indeed identical ($t_4 z_4^{-1} = t_4 n_4 = t_1$), while the spectral phasor diagrams for complex reflection coefficients (solid red lines) are different. To setup a numerical validation test, the retrieved effective BA parameters are then used in

$$h_{13,j} = \frac{1}{2}\left(h_j - \iota(k_0 n)^{-1}\partial h_j/\partial x\right)$$

$$h_{31,j} = \frac{1}{2}\left(h_j + \iota(k_0 n)^{-1}\partial h_j/\partial x\right)$$

$$e_j = z_0(z_{13}h_{13,j} - z_{31}h_{31,j}) \tag{31}$$

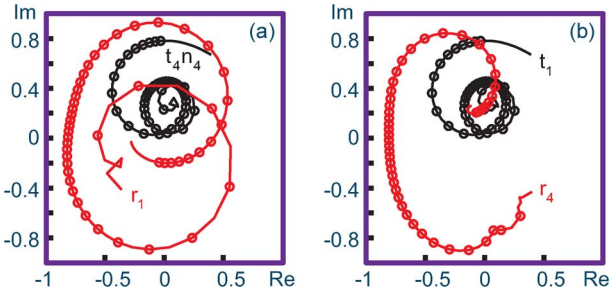

Fig. 3. *Spectral phasor diagrams for a metamagnetic sample: (a) front-side and (b) back-side illumination substrate-normalized complex transmission coefficients and complex reflection coefficients from a nanostructured metamagnetic (SHA, solid lines) compared to those from the homogenized slab (FEM, circles).*

and in simpler equivalents of (26) for reciprocal media

$$d_j = c_0^{-1}\left[(z_{13}\varepsilon + u)h_{13,j} - (z_{31}\varepsilon - u)h_{31,j}\right]$$

$$b_j = \mu_0\left[(\mu - z_{13}u)h_{13,j} + (\mu + z_{31}u)h_{31,j}\right]. \qquad (32)$$

First, (32) is used as auxiliary differential equations (ADE) in the finite element method (FEM) domain, so that the local, spatially dependent material parameters inside the effective BA slab are defined by (27). Once the equations for $\tilde{\mu}_j$ and $\tilde{\varepsilon}_j$ are set, the scalar wave equation for the transverse magnetic field is then solved self-consistently. The matching r, t FEM results for the homogenized slab, equivalent to a given metamagnetic, are shown as red and black circles in Fig. 3(a) and (b).

Further insight into the performance of the bianisotropic MM may be obtained by examining the relative permittivity $(\tilde{\varepsilon})$ and permeability $(\tilde{\mu})$ (27), within the effective slab. Fig. 4 shows $\tilde{\varepsilon}$ and $\tilde{\mu}$ as a function of position in the slab for both front-side and back-side illumination, both with and without the glass substrate.

We also studied the effective parameters of a 2-D NIM [7], as shown in Fig. 1(b). Again, for simplicity, we have removed the ITO layer from the simulations $\delta_{\mathrm{ITO}} = 0$. We used a previously optimized geometry of $\{p, w, \delta_1, \delta_{\mathrm{Ag}}, \delta_{\mathrm{S}}\} = \{324, 168, 20, 46, 68\}$ [nm]. Spectra and r, t coefficients from SHA are shown in Fig. 5(a), (e), and (f), and the retrieved effective optical parameters are shown in Fig. 5(b)–(d). Again we see that the effective homogenized slab, also Fig. 5(e) and (f), matches the SHA results of the structured geometry.

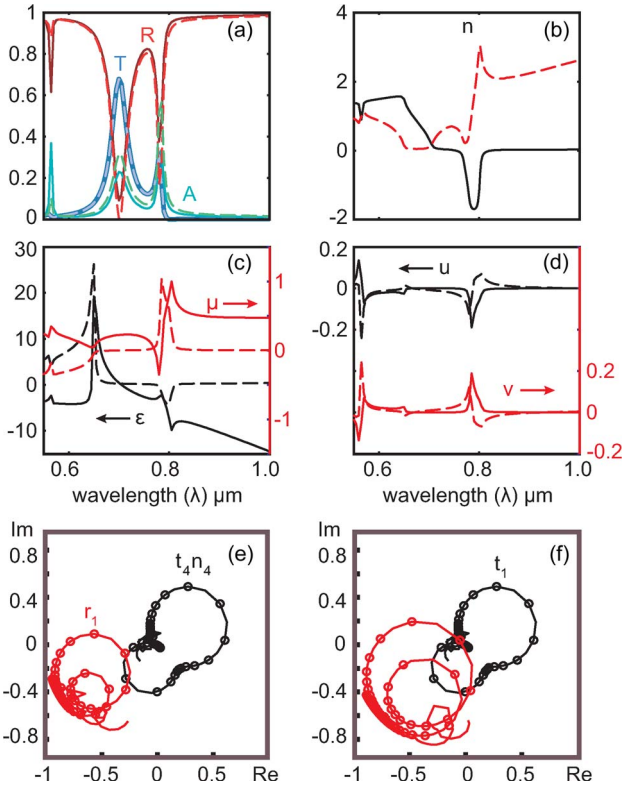

Fig. 5. *2-D NIM. (a) TM spectra (solid lines: front-side illumination; dashed: backside), (b) retrieved index of refraction $[n]$ [for (b)–(f), solid: real part, dashed: imaginary part], (c) retrieved permittivity $[\varepsilon]$ and permeability $[\mu]$, (d) retrieved bianisotropy $[u, v]$, (e) front-side and (f) back-side illumination complex reflection (r: red) and transmission (t: black) coefficients from metamagnetic (SHA: solid lines) compared to those from the homogenized BA slab (FEM: circles) (red: real part; black: imaginary part).*

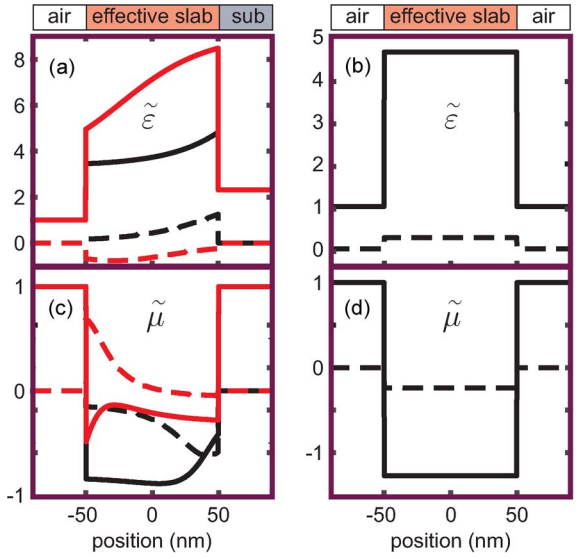

Fig. 4. *Relative optical properties as a function of position for a metamagnetic grating equivalent slab on a glass substrate: (a) $\tilde{\varepsilon}$ and (c) $\tilde{\mu}$ and in air: (b) $\tilde{\varepsilon}$ and (d) $\tilde{\mu}$. Illumination is at 700 nm from front side (black) and back side (red) (solid: real; dashed: imaginary).*

We also analyze the relative permittivity $(\tilde{\varepsilon})$ and permeability $(\tilde{\mu})$ within the 2-D NIM equivalent slab, shown in Fig. 6, which again shows that the presence of the substrate induces an asymmetric optical response within the effective medium. Figs. 4(b) and (d) and 6(b) and (d) confirm that for any center-symmetric unit cell arranged of reciprocal elemental materials, not only the optical response is reciprocal, but it is also nonbianisotropic $(u, v \equiv 0)$, and therefore $\tilde{\varepsilon} = \varepsilon$, $\tilde{\mu} = \mu$.

The high optical loss (large imaginary refractive index) in these materials warrants the use of a gain medium to enhance the transmission of the sample, and has been discussed at length elsewhere [10]. Therefore, we have also analyzed a 2-D NIM structure, Fig. 1(b), where the dielectrics (alumina and silica) have both been replaced with a simple gain medium.

The permittivity of the simple gain medium is defined using a Cauchy model to simulate the dielectric host (set equivalent to alumina), and uses a negative Lorentz

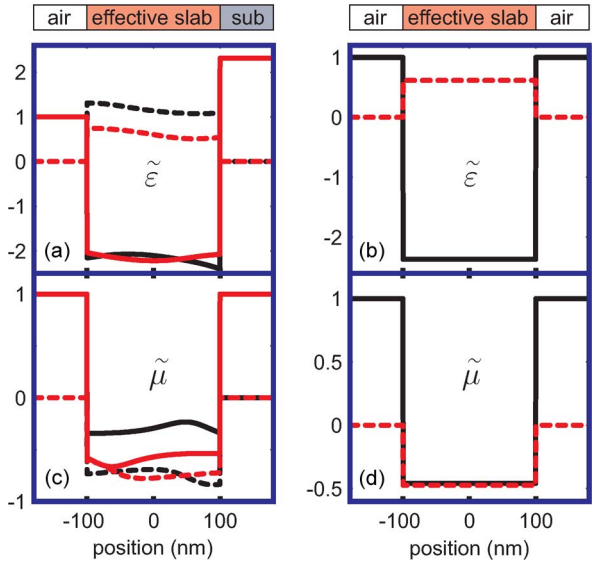

Fig. 6. *Relative optical properties as a function of position for a 2-D NIM equivalent slab on a glass substrate: (a) $\tilde{\varepsilon}$ and (b) $\tilde{\mu}$ and in air: (c) $\tilde{\varepsilon}$ and (d) $\tilde{\mu}$. Illumination is at 700 nm from front side (black) and back side (red) (solid: real; dashed: imaginary).*

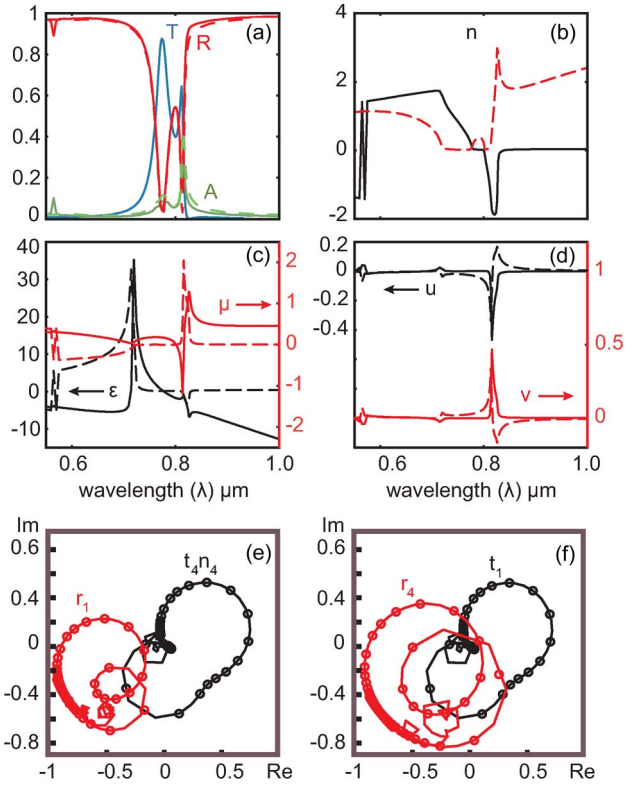

Fig. 7. *2-D NIM with gain. (a) TM spectra (solid lines: front-side illumination; dashed: backside), (b) retrieved index of refraction $[n]$ [for (b)–(f), solid: real part, dashed: imaginary part], (c) retrieved permittivity $[\varepsilon]$ and permeability $[\mu]$, (d) retrieved bianisotropy $[u, v]$, (e) front-side and (f) back-side illumination complex reflection (r: red) and transmission (t: black) coefficients from metamagnetic (SHA: solid lines) compared to those from the homogenized slab (FEM: circles) (red: real; black: imaginary).*

oscillator (resulting in a negative imaginary n), with an amplitude such that the peak gain is 1000 cm^{-1} centered at 780 nm with a width of 100 nm, to simulate the effect of a stimulated emission transition in an embedded dye. This results in a static frequency-domain model for gain, which will of course not represent many transient and intensity-dependent effects, but which is sufficient to represent the effect of a negative imaginary permittivity, with a realistic amplitude and spectral dependence, on the effective medium parameters.

Again, spectra and r, t coefficients from SHA are shown in Fig. 7(a), (e), and (f), compared to the BA slab Fig. 7(e) and (f), and the retrieved effective optical parameters are shown in Fig. 7(b)–(d). Although the resonances are red-shifted, due to replacing silica $n = 1.5$ with an alumina-like gain material $\text{Re}(n) \cong 1.62$ and narrowed slightly from the dielectric case, we see that the retrieved imaginary refractive index is lower near the wavelength with peak negative refractive index. With no gain, $\text{Im}(n) = 0.25$ at 775 nm, whereas with gain, $\text{Im}(n) = 0.06$ at 810 nm.

VI. SUMMARY AND FUTURE WORK

In this paper, we presented an approach to the BA homogenization of optical MMs (including deposited on a covered substrate) and discussed several techniques for validating the retrieved effective parameters of these nanostructures. The theoretical fundamentals of BA homogenization are developed using the transfer matrix formalism applied to passive and active optical MMs. First, we use (5), (8), and (10) to develop the sequence of conversion from parameters z_{13}, n_{13} and z_{31}, n_{31}— which could be obtained from experiment—to unknown BA parameters u, v, μ, and ε. Then, we compare the transfer matrix with unknown parameters z_{13}, n_{13} and z_{31}, n_{31} defined in (15) with the same transfer matrix that could be obtained from the experimental data in (17). The comparison resulted in formulas (22) and (23), connecting z_{13}, n_{13}, z_{31}, n_{31}, with complex transmission (t_4, t_1) and reflection (r_1, r_4) coefficients available from optical characterization of a given MM sample. That concludes the development of the homogenization approach.

Then, we focus our theoretical development and numerical validation solely at the practical case of reciprocal media for which easier analysis is possible. The initial reciprocity condition $T_1 = T_4$ is satisfied only if $u = -v$, and the propagation constants do not depend on the illumination side, i.e., $s_{13} = s_{31} \to s$ and $n_{13} = n_{31} \to n$ and simpler (28), (29), and (30) could be used to determine the BA effective parameters of the MM.

This approach was applied to a simple metamagnetic grating and a 2-D NIM. Coefficients t_4, t_1, r_1, r_4 were

obtained from SHA simulations, and the retrieved optical parameters were presented here. This retrieval approach is shown to reproduce the expected electrical and magnetic resonances, in addition to significant BA. Further, FEM simulations using the effective parameters in a homogeneous "slab" accurately reproduce the complex coefficients of the metal-dielectric MM. These homogeneous FEM simulations are also analyzed to show the distribution of the relative field-ratio parameters $\tilde{\varepsilon}, \tilde{\mu}$. This result shows that the substrate induced asymmetry (front-side versus back-side illumination) of the field within the slab results in asymmetric values for $\tilde{\varepsilon}, \tilde{\mu}$, as opposed to a symmetric geometry with no substrate, which has constant $\tilde{\varepsilon}, \tilde{\mu}$ values.

Indeed the presence of the substrate is seen to have a significant effect on the retrieved values, and therefore on the performance and BA of the MM. In essence, the retrieved effective parameters are certainly nonlocal, embedding the influence of substrate–superstrate environment. We would conclude that retrieval and discussion of MM bianisotropic optical parameters cannot be separated from substrate–superstrate media and incidence direction.

A more advanced BA-based characterization method will be used as an advantageous tool for the studies of the effective angular-dependent models of MMs. ■

Acknowledgment

The authors would like to thank the reviewers for several vital suggestions. A. V. Kildishev would also like to thank N. Engheta for valuable discussions.

REFERENCES

[1] U. K. Chettiar, S. Xiao, A. V. Kildishev, W. Cai, H. K. Yuan, V. P. Drachev, and V. M. Shalaev, "Optical metamagnetism and negative-index metamaterials," *MRS Bull.*, vol. 33, pp. 921–926, Oct. 2008.

[2] S. G. Rautian, "Reflection and refraction at the boundary of a medium with negative group velocity," *Physics-Uspekhi*, vol. 51, pp. 981–988, Oct. 2008.

[3] D. R. Smith, S. Schultz, P. Markos, and C. M. Soukoulis, "Determination of effective permittivity and permeability of metamaterials from reflection and transmission coefficients," *Phys. Rev. B*, vol. 65, May 15, 2002, 195104.

[4] W. B. Weir, "Automatic measurement of complex dielectric-constant and permeability at microwave-frequencies," *Proc. IEEE*, vol. 62, no. 1, pp. 33–36, Jan. 1974.

[5] "Comments on 'Automatic measurement of complex dielectric-constant and permeability at microwave-frequencies'," *Proc. IEEE*, vol. 63, no. 1, pp. 203–205, Jan. 1975.

[6] W. S. Cai, U. K. Chettiar, H. K. Yuan, V. C. de Silva, A. V. Kildishev, V. P. Drachev, and V. M. Shalaev, "Metamagnetics with rainbow colors," *Opt. Exp.*, vol. 15, pp. 3333–3341, Mar. 2007.

[7] U. K. Chettiar, A. V. Kildishev, T. A. Klar, and V. M. Shalaev, "Negative index metamaterial combining magnetic resonators with metal films," *Opt. Exp.*, vol. 14, pp. 7872–7877, Aug. 21, 2006.

[8] C. Enkrich, M. Wegener, S. Linden, S. Burger, L. Zschiedrich, F. Schmidt, J. F. Zhou, T. Koschny, and C. M. Soukoulis, "Magnetic metamaterials at telecommunication and visible frequencies," *Phys. Rev. Lett.*, vol. 95, 2005, 203901.

[9] A. V. Kildishev, W. S. Cai, U. K. Chettiar, H. K. Yuan, A. K. Sarychev, V. P. Drachev, and V. M. Shalaev, "Negative refractive index in optics of metal-dielectric composites," *J. Opt. Soc. Amer. B—Opt. Phys.*, vol. 23, pp. 423–433, Mar. 2006.

[10] T. A. Klar, A. V. Kildishev, V. P. Drachev, and V. M. Shalaev, "Negative-index metamaterials: Going optical," *IEEE J. Sel. Topics Quantum Electron.*, vol. 12, no. 6, pt. 1, pp. 1106–1115, Nov./Dec. 2006.

[11] S. Linden, C. Enkrich, M. Wegener, J. F. Zhou, T. Koschny, and C. M. Soukoulis, "Magnetic response of metamaterials at 100 terahertz," *Science*, vol. 306, pp. 1351–1353, Nov. 19, 2004.

[12] G. Shvets and Y. A. Urzhumov, "Negative index meta-materials based on two-dimensional metallic structures," *J. Opt. A—Pure Appl. Opt.*, vol. 8, pp. S122–S130, Apr. 2006.

[13] S. M. Xiao, U. K. Chettiar, A. V. Kildishev, V. Drachev, I. C. Khoo, and V. M. Shalaev, "Tunable magnetic response of metamaterials," *Appl. Phys. Lett.*, vol. 95, Jul. 20, 2009, 033115.

[14] H.-K. Yuan, U. K. Chettiar, W. Cai, A. V. Kildishev, A. Boltasseva, V. P. Drachev, and V. M. Shalaev, "A negative permeability material at red light," *Opt. Exp.*, vol. 15, pp. 1076–1083, 2007.

[15] S. Zhang, W. J. Fan, B. K. Minhas, A. Frauenglass, K. J. Malloy, and S. R. J. Brueck, "Midinfrared resonant magnetic nanostructures exhibiting a negative permeability," *Phys. Rev. Lett.*, vol. 94, Jan. 28, 2005, 037402.

[16] V. A. Podolskiy, A. K. Sarychev, E. E. Narimanov, and V. M. Shalaev, "Resonant light interaction with plasmonic nanowire systems," *J. Opt. A—Pure Appl. Opt.*, vol. 7, pp. S32–S37, Feb. 2005.

[17] A. V. Kildishev and V. M. Shalaev, "Engineering space for light via transformation optics," *Opt. Lett.*, vol. 33, pp. 43–45, Jan. 1, 2008.

[18] R. A. Depine and A. Lakhtakia, "A new condition to identify isotropic dielectiric-magnetic materials displaying negative phase velocity," *Microw. Opt. Technol. Lett.*, vol. 41, pp. 315–316, May 20, 2004.

[19] R. W. Ziolkowski and E. Heyman, "Wave propagation in media having negative permittivity and permeability," *Phys. Rev. E*, vol. 64, Nov. 2001, 056625.

[20] V. M. Shalaev, "Optical negative-index metamaterials," *Nature Photon.*, vol. 1, pp. 41–48, Jan. 2007.

[21] J. B. Pendry, "Negative refraction makes a perfect lens," *Phys. Rev. Lett.*, vol. 85, p. 3966, 2000.

[22] V. G. Veselago, "Electrodynamics of substances with simultaneously negative values of Sigma and Mu," *Soviet Physics Uspekhi-USSR*, vol. 10, p. 509, 1968.

[23] A. J. Hoffman, L. Alekseyev, S. S. Howard, K. J. Franz, D. Wasserman, V. A. Podolskiy, E. E. Narimanov, D. L. Sivco, and C. Gmachl, "Negative refraction in semiconductor metamaterials," *Nature Mater.*, vol. 6, pp. 946–950, Dec. 2007.

[24] D. R. Smith and D. Schurig, "Electromagnetic wave propagation in media with indefinite permittivity and permeability tensors," *Phys. Rev. Lett.*, vol. 90, Feb. 21, 2003, 077405.

[25] D. R. Smith, D. Schurig, J. J. Mock, P. Kolinko, and P. Rye, "Partial focusing of radiation by a slab of indefinite media," *Appl. Phys. Lett.*, vol. 84, pp. 2244–2246, Mar. 29, 2004.

[26] R. Wangberg, J. Elser, E. E. Narimanov, and V. A. Podolskiy, "Nonmagnetic nanocomposites for optical and infrared negative-refractive-index media," *J. Opt. Soc. Amer. B—Opt. Phys.*, vol. 23, pp. 498–505, Mar. 2006.

[27] J. Yao, Z. W. Liu, Y. M. Liu, Y. Wang, C. Sun, G. Bartal, A. M. Stacy, and X. Zhang, "Optical negative refraction in bulk metamaterials of nanowires," *Science*, vol. 321, pp. 930–930, Aug. 15, 2008.

[28] J. B. Pendry, D. Schurig, and D. R. Smith, "Controlling electromagnetic fields," *Science*, vol. 312, pp. 1780–1782, Jun. 23, 2006.

[29] A. V. Kildishev, W. Cai, U. K. Chettiar, and V. M. Shalaev, "Transformation optics: Approaching broadband electromagnetic cloaking," *New J. Phys.*, vol. 10, Nov. 27, 2008, 115029.

[30] S. A. Zhang, W. J. Fan, N. C. Panoiu, K. J. Malloy, R. M. Osgood, and S. R. J. Brueck, "Optical negative-index bulk metamaterials consisting of 2D perforated metal-dielectric stacks," *Opt. Exp.*, vol. 14, pp. 6778–6787, Jul. 24, 2006.

[31] C. M. Soukoulis, S. Linden, and M. Wegener, "Negative refractive index at optical wavelengths," *Science*, vol. 315, pp. 47–49, Jan. 5, 2007.

[32] W. Q. Chen, M. D. Thoreson, S. Ishii, A. V. Kildishev, and V. M. Shalaev, "Ultra-thin ultra-smooth and low-loss silver films on a germanium wetting layer," *Opt. Exp.*, vol. 18, pp. 5124–5134, Mar. 1, 2010.

[33] V. J. Logeeswaran, N. P. Kobayashi, M. S. Islam, W. Wu, P. Chaturvedi, N. X. Fang, S. Y. Wang, and R. S. Williams, "Ultrasmooth silver thin films deposited with a germanium nucleation layer," *Nano Lett.*, vol. 9, pp. 178–182, 2008.

[34] R. Marques, F. Medina, and R. Rafii-El-Idrissi, "Role of bianisotropy in negative permeability and left-handed metamaterials," *Phys. Rev. B*, vol. 65, Apr. 1, 2002, 144440.

[35] C. E. Kriegler, M. S. Rill, S. Linden, and M. Wegener, "Bianisotropic photonic metamaterials," *IEEE J. Sel. Topics Quantum Electron.*, vol. 16, no. 2, pp. 367–375, Mar.–Apr. 2010.

[36] X. Chen, B. I. Wu, J. A. Kong, and T. M. Grzegorczyk, "Retrieval of the effective constitutive parameters of bianisotropic metamaterials," *Phys. Rev. E*, vol. 71, Apr. 2005, 046610.

[37] X. D. Chen, B. I. Wu, J. A. Kong, and T. M. Grzegorczyk, "Erratum: Retrieval of the effective constitutive parameters of bianisotropic metamaterials (vol 71, pg 046610, 2005)," *Phys. Rev. E*, vol. 73, Jan. 2006, 019905.

[38] Z. Ku, K. M. Dani, P. C. Upadhya, and S. R. Brueck, "Bianisotropic negative-index metamaterial embedded in a symmetric medium," *J. Opt. Soc. Amer. B*, vol. 26, pp. B34–B38, 2009.

[39] M. S. Rill, C. Plet, M. Thiel, I. Staude, G. Von Freymann, S. Linden, and M. Wegener, "Photonic metamaterials by direct laser writing and silver chemical vapour deposition," *Nature Mater.*, vol. 7, pp. 543–546, Jul. 2008.

[40] D. A. Powell and Y. S. Kivshar, "Substrate-induced bianisotropy in metamaterials," *Appl. Phys. Lett.*, vol. 97, 2010, 091106.

[41] S. M. Xiao, V. P. Drachev, A. V. Kildishev, X. J. Ni, U. K. Chettiar, H. K. Yuan, and V. M. Shalaev, "Loss-free and active optical negative-index metamaterials," *Nature*, vol. 466, p. 735-U6, Aug. 5, 2010.

[42] A. V. Kildishev and U. K. Chettiar, "Cascading optical negative index metamaterials," *Appl. Comput. Electromagn. Soc. J.*, vol. 22, pp. 172–183, Mar. 2007.

[43] X. Ni, Z. Liu, F. Gu, M. G. Pacheco, J. D. Borneman, and A. V. Kildishev, "PhotonicsSHA-2D: Modeling of single-period multilayer optical gratings and metamaterials," 2009, DOI: 10254/nanohub-r6977.9.

ABOUT THE AUTHORS

Alexander V. Kildishev (Senior Member, IEEE) received the M.S. degree in electrical engineering (honors) from the Kharkov State Polytechnical University (KSPU), Ukraine, and the Ph.D. degree in electrical engineering from KSPU in 1996.

He is a Principal Research Scientist at the Birck Nanotechnology Center, School of Electrical and Computer Engineering, Purdue University, West Lafayette, IN. He leads the development of simulation methods and software tools for applied electromagnetics and multiphysics simulations. Before joining Purdue University, he was working as the Head of Laboratory at the Magnetism Division of the National Academy of Sciences in the Ukraine. Currently, his research interests are in the modeling of nanophotonics devices, optical metamaterials, and transformation optics. His publications include four book chapters, four patents, more than 80 articles in peer-reviewed journals, with more than 2000 citations, and more than 30 invited seminar and conference talks.

Dr. Kildishev is a member of the Optical Society of America (OSA), the International Society for Optics and Photonics (SPIE), the Society for Industrial and Applied Mathematics (SIAM), and the Applied Computational Electromagnetics Society (ACES).

Joshua D. Borneman received the M.S. degree in physics and the Ph.D. degree in electrical and computer engineering (working with Prof. V. M. Shalaev's group) from Purdue University, West Lafayette, IN, in 2004 and 2010, respectively.

He is currently an Engineer for the Navy at NSWC Crane Division, Crane, IN, working on electro-optic science and technology projects. His interests include characterization and simulation of metamaterials and nonlinear optics. He has also worked as a Mathematics Instructor at Purdue University, and as a Technical Intern for Intel Corporation.

Dr. Borneman has been a member of the Optical Society of America (OSA) since 2004.

Xingjie Ni received the B.S. degree in engineering physics and the M.S. degree in automation from Tsinghua University, Beijing, China, in 2005 and 2007, respectively. He is currently working as a Research Assistant towards the Ph.D. degree in electrical and computer engineering in Prof. V. M. Shalaev's group at the Birck Nanotechnology Center, School of Electrical and Computer Engineering, Purdue University, West Lafayette, IN. He is also working towards the M.S. degree in computer science under the supervision of Prof. A. Sameh at Purdue University.

His current research interests include modeling and characterization of metamatertials, transformation optics devices, and computational electromagnetics.

Mr. Ni is a member of the Optical Society of America (OSA).

Vladimir (Vlad) M. Shalaev (Fellow, IEEE) received the M.S. degree in physics (with highest distinction) and the Ph.D. degree in physics and mathematics from Krasnoyarsk State University, Russia, in 1979 and 1983, respectively.

He is the Robert and Anne Burnett Professor of Electrical and Computer Engineering and Professor of Biomedical Engineering at Purdue University, West Lafayette, IN, and specializes in nanophotonics, plasmonics, and optical metamaterials. He authored three books, 21 book chapters, and over 300 research publications, in total.

Prof. Shalaev received several awards for his research in the field of nanophotonics and metamaterials, including the Max Born Award of the Optical Society of America (OSA) for his pioneering contributions to the field of optical metamaterials and the Willis E. Lamb Award for Laser Science and Quantum Optics. He is a Fellow of the American Physical Society (APS), the International Society for Optics and Photonics (SPIE), and the Optical Society of America (OSA).

Vladimir P. Drachev graduated from Novosibirsk State University, Russia and received the Ph.D. degree in experimental physics from the Institute of Semiconductor Physics and the Institute of Automation and Electrometry, Russian Academy of Sciences (RAS), Moscow, Russia, in 1995.

He has been a Senior Research Scientist with the Birck Nanotechnology Center and School of Electrical and Computer Engineering, Purdue University, West Lafayette, IN, since 2002. In 1999–2001, he worked as a Visiting Scientist at New Mexico State University. His current research interests include optics and nonlinear optics, nonlinear spectroscopy of nanomaterials, spectroscopy of metal-molecule complexes, biosensing, nano-optics, nanofabrication, plasmonics, and metamaterials.

Dr. Drachev has been granted several awards from the International Science Foundation, and the Ostrovskii award (1997) from Ioffe Institute of Russian Academy of Sciences (RAS), St. Petersburg, Russia.